Distribution of some active elements in primary graphite precipitates

K. Theuwissen*, T. Duguet, J. Esvan and J. Lacaze

The distributions of cerium and oxygen in the matrix and in graphite precipitates of a pure Fe–C–Ce cast iron sample have been studied using scanning Auger microscopy. It is shown that there is no accumulation of any element at the graphite-matrix interface. Cerium was detected in some cases in spheroidal graphite precipitates, most often associated with oxygen. Various non-spheroidal graphite precipitates proved to contain cerium and oxygen suggesting a correlation between cerium content and graphite degeneracy.

Keywords: Ductile iron, Graphite growth, Auger analysis, Cerium, oxygen

Introduction

As does magnesium, cerium and other rare earth el ements are known to be graphite spheroidizers in cast irons, meaning that added at minute level in the melt before casting they lead to graphite precipitating as disconnected spheres or nodules instead of interconnected lamellae. Distribution of these elements in graphite has long been studied but most generally with analytical means having poor spatial and/or analytical resolution. In an attempt to describe cerium distribution within graphite nodules, Hillert and Lindlblom[1] used autoradiography and found cerium absorbed in the bulk of graphite nodules. This led them to suggest that this element adsorbs at the graphite surface so as to favour its growth along the *c* direction, and proposed this occurs by growth around screw dislocations. Although the conclusions of this work have been criticised by Olette *et al.*[2] because of the poor spatial resolution associated to autoradiography of cerium, Minkoff and Nixon[3] arrived to similar conclusions by analysing their results on lanthanum distribution between graphite and cast iron melt. Attempts to use secondary ion mass spectroscopy[4] with the same goal also showed limits in practical spatial and analytical resolutions. The present work attempts to analyse the distribution of Ce in pure Fe–C–Ce alloys by means of scanning Auger microscopy (SAM), which has seldom been used to study cast irons[5,6], so as to understand how cerium could affect graphite growth.

Experimental

Small pieces of metallic Ce were placed at the bottom of a graphite crucible (ALPHA AR6247, for chemical analysis). They were covered with pure Fe with a Ce/Fe ratio of 2 wt.% and a graphite lid was used to cover the sample. The graphite crucible was then introduced in an experimental set-up described in previous work[7] in order to undergo a medium vacuum (10^{-3} mbar) heat treatment. In the first step, the sample was heated to 1350 °C and maintained at that temperature for 15 min so as to enrich the iron with carbon leading to a carbon saturated Fe-rich liquid. The following step consisted in cooling the sample to 1180 °C and holding it for 30 min for primary graphite nucleation and growth. Finally, the sample was quenched with an air blowing-device and cut for metallographic observation of the cross section.

The sample was then analysed using a LEO 435VP scanning electron microscope and a Thermo Scientific Microlab 350 SAM. Auger analyses were performed at a primary electron energy of 10 kV. Sample's surface was cleaned by ion sputtering (Ar^+, 3 kV, 1.5 μA) prior to measurements and observations. Ce peaks appearing at low energies (between 64 and 116 eV) were the most intense, with the maximum at kinetic energy 82 eV. They were used to evidence the presence of Ce since the other less intense peaks (563–788 eV) overlap with the Fe LMM peaks (550 and 703 eV). It is important to note that the relative sensitivity of Fe is approximately three times higher than that of Ce MNN peaks, therefore the latter can hardly be used to identify Ce in the presence of Fe. Auger mapping was performed in snapshot mode, where the 6 channeltrons are used to detect the peak and background signals separately. First, the channeltrons are tuned within the energy range of the peak (signal P) of interest and then within an energy range which defines the background intensity (B). Images shown in the present work correspond to the ratio (P−B)/B, which reduces considerably any possible topography contrast and reveals better the chemical contrast than P-B. For the conditions used, the expected detection limit ranges between 0.1 and 0.5 % while the spatial resolution (in spot mode) is 30 nm on the surface and 10 nm in depth.

Results and discussion

Figure 1*a* is a backscattered electron image of the sample, showing the shape and distribution of graphite precipitates that appear in dark contrast and the areas where the figures

CIRIMAT, CNRS-Université de Toulouse, ENSIACET, BP 44362, 31030, Toulouse cedex 4, France

*Corresponding author, email koenraad.theuwissen@ensiacet.fr

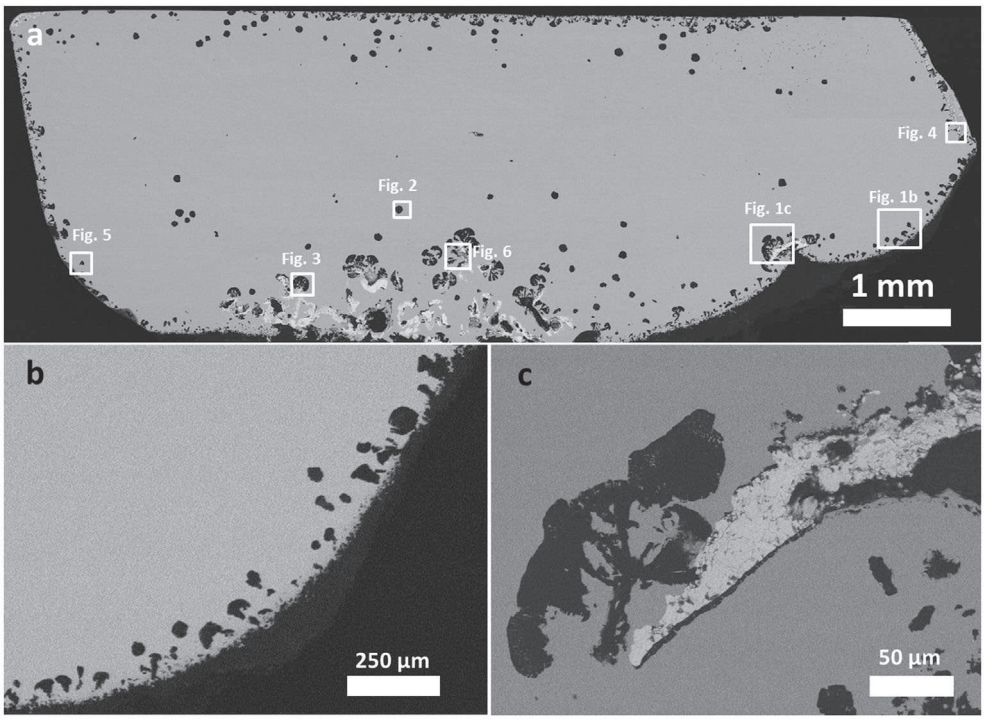

1 Photomontage of backscattered electron images showing an overview of the sample and the areas analysed in this study *a*; graphite precipitates at the edge of the sample *b* and close to Ce-rich particles *c*

presented in this study are located. Most of these precipitates are found close to the edges of the sample, that is to say the former crucible walls. Upon cooling to 1180 °C, primary graphite precipitates nucleated and grew at the crucible walls, then eventually detached from the walls and settled and grew freely in the liquid during the holding stage. When close or attached to the walls, these precipitates appear as cones, (Fig. 1*b*) which can be compared to the conical sectors that are usually observed in sections of complete graphite spheroids. Those precipitates that detached from the walls transformed progressively to complete spheroids when settling.

The bright particles found in the sample were analysed with energy dispersive X-ray analysis and proved to contain mainly cerium and oxygen. These particles are certainly cerium oxides: cerium is known to have a high affinity for oxygen and to form stable oxides such as Ce_2O_3 and CeO_2 which are likely to form in the pressure and temperature ranges used in this study. These were mostly found at the bottom of the sample where metallic cerium was added prior to melting. Large isolated sectors and other degenerate carbon morphologies were often found close to these Ce-rich particles, and in some cases graphite was observed to surround their outer surface as in Fig. 1*c*. The size of the sectors as well as the graphite deposit along the Ce-rich precipitates suggest that these cerium oxides can act as nucleating particles for graphite.

Graphite precipitates formed on the crucible walls and on Ce-rich precipitates appear very similar, consisting of sectors very much alike those observed in fully formed spherulites, though separated from each other. Cerium thus forces the overall growth of graphite to occur along its ***c*** direction. At the same time, it appears to limit growth along the ***a*** direction as the observed sectors do not apparently expand laterally to fill the space, and rather stop expanding and thus let significant space to appear between neighbouring sectors grown from the same "center". Graphite precipitates found in the bulk of the sample, that are expected to have detached from the crucible walls, appear as spheroids that are more or less filled with graphite, though many matrix inclusions could be observed at high magnifications. This may mean that during the settling process, cerium atoms attached to the graphite/liquid interface have diffused to the bulk liquid, thus allowing for the filling of the spheroids with carbon.

It has been suggested that morphological modification of graphite occurs mainly through adsorption of foreign elements on the graphite's outer surfaces[8–10], e.g. oxygen and sulphur that favour lamellar growth on the one hand, magnesium, cerium and other spheroidising elements on the other hand. Accordingly, it seemed of interest to study the chemical composition of graphite-matrix interfaces, but Auger survey scans showed no build-up of any elements at these locations, though cerium and oxygen were detected in small matrix intrusions at the periphery of graphite spheroids as shown in Fig. 2.

The same observations were made on matrix inclusions in degenerate graphite precipitates as shown in Fig. 3. This so-called exploded graphite precipitate in Fig. 3*a* developed close to Ce-rich particles seen in the upper-left part of the micrograph in Fig. 3*a*, and the cerium map of Figure 3b was produced by collecting spectra every 0.2 µm within the white frame shown in Fig. 3*a*. It is important to note that these spectra were taken immediately after an ion sputtering stage which was carried out to eliminate surface contamination. The values close to the CeNO1 energy defined the peak (P) to be considered for cerium. Therefore, the detectors were centred around 84 eV, resulting in a peak energy range between 82.9 and 85.1 eV. To define the background intensities, the detectors were centred around 93 eV resulting in a background energy (B) ranging from 91.8 to 94.2 eV. The values of P and B were used to normalise the signal so as to eliminate any topography-related effects. The map in Fig. 3*b* shows that cerium was certainly present in both the inclusion and graphite, though no quantitative conclusion could be drawn as the intensity of the signal on the matrix from which it originates.

The map highlights two Ce-rich spots in the lower left corner of Fig. 3*b*. In order to confirm this observation, Auger

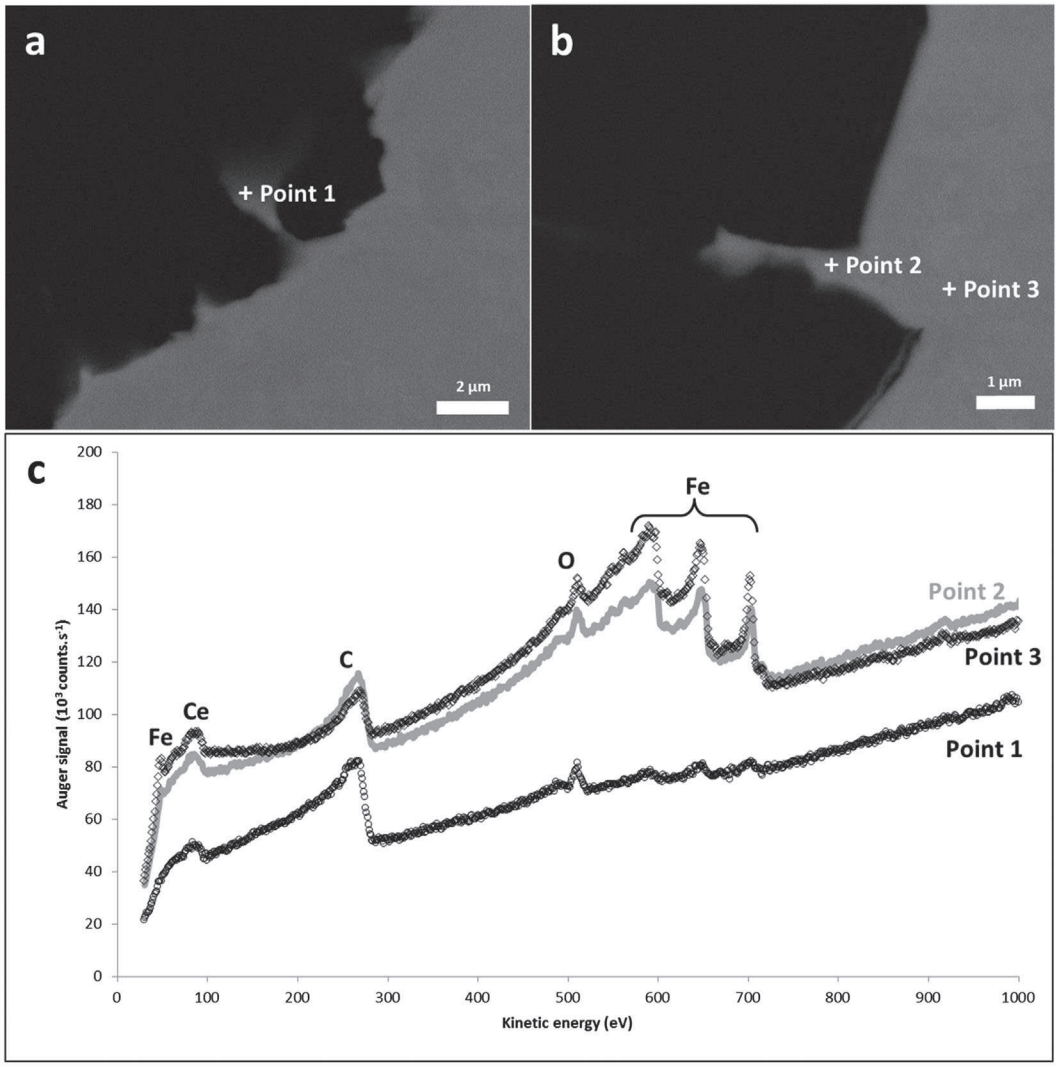

2 Location of point spectra (*a* and *b*) and associated spectra *c* where Ce and O are detected in matrix intrusions at the periphery of graphite precipitates

spectra were taken in points 1, 2 and 3 in Fig. 3*c* across the bottom extremity of the Fe-rich inclusion. The results are reported in Fig. 3*d* and reveal a Ce peak at 84 eV in all three points, as well as oxygen peaks around 509 eV. The spectrum corresponding to point 3 shows slight Fe-peaks at 610, 650 and 703 eV, suggesting that this element is also present within graphite at point 3, while it is not in point 1. This suggests that point 1 corresponds to a cerium oxide which may have formed because of oxygen and cerium rejection during solidification of graphite and/or the iron inclusion, while point 3 would most probably be associated to an even distribution of oxygen, iron and cerium in graphite. Further, a cerium signal is detected in point 2 which shows this element is definitely present in the iron-rich inclusion, though no quantitative conclusion could be made, in particular concerning the relative amount of cerium in graphite and the iron-rich inclusion.

From these results it is seen that cerium, combined with oxygen, can be found in graphite and the question rises as to whether their presence in the precipitates is directly related to the spheroidisation process. Survey scans were performed in parts of seven graphite spheroids, but the detection of Ce was not consistent as it was observed only in some cases.

It seemed sensible to assume that the incorporation of cerium in graphite precipitates was more likely to occur at locations which were close to Ce-rich particles such as the ones shown in Fig. 4*a*. Spectra were thus collected at four points along the line in Fig. 4*b* going from a cerium-rich particle (point 1) to a graphite precipitate (points 2–4). All four spectra show cerium and oxygen peaks confirming the presence of cerium within the graphite precipitate.

The possibility that the elements detected in graphite came from sample preparation (i.e. dragging of small Ce-rich particles during polishing) was considered hence a depth profile was performed. Survey spectra were collected after successive Ar^+ sputtering stages of a graphite nodule shown in Fig. 5*a*. The successive spectra are superimposed in Fig 5*b* and show that foreign elements (cerium, oxygen and iron) are detected before and after etching.

Following this result, emphasis was put on the graphite precipitates found near the cerium-rich particles. These seem to have undergone incomplete spheroidisation and their morphology can be qualified as degenerate. Auger analysis showed a systematic presence of cerium and oxygen as well as iron in these precipitates as shown in Fig. 6.

Observations of foreign elements in graphite have been reported by several authors,[11–13] mainly for spheroidal graphite. From the detection of Ce and O within graphite, it has been claimed that compounds such as Ce_2O_3 can be

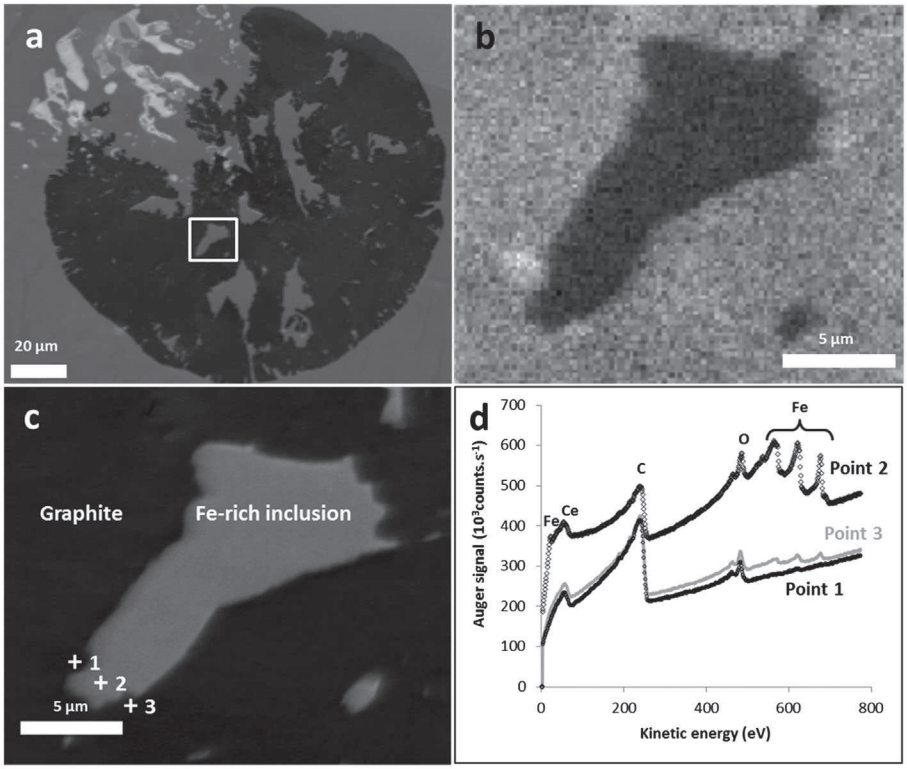

3 SEM micrograph of an exploded graphite precipitate *a*, Ce Auger map in the area squared in a *b*, location of the spots *c* and corresponding Auger spectra *d*

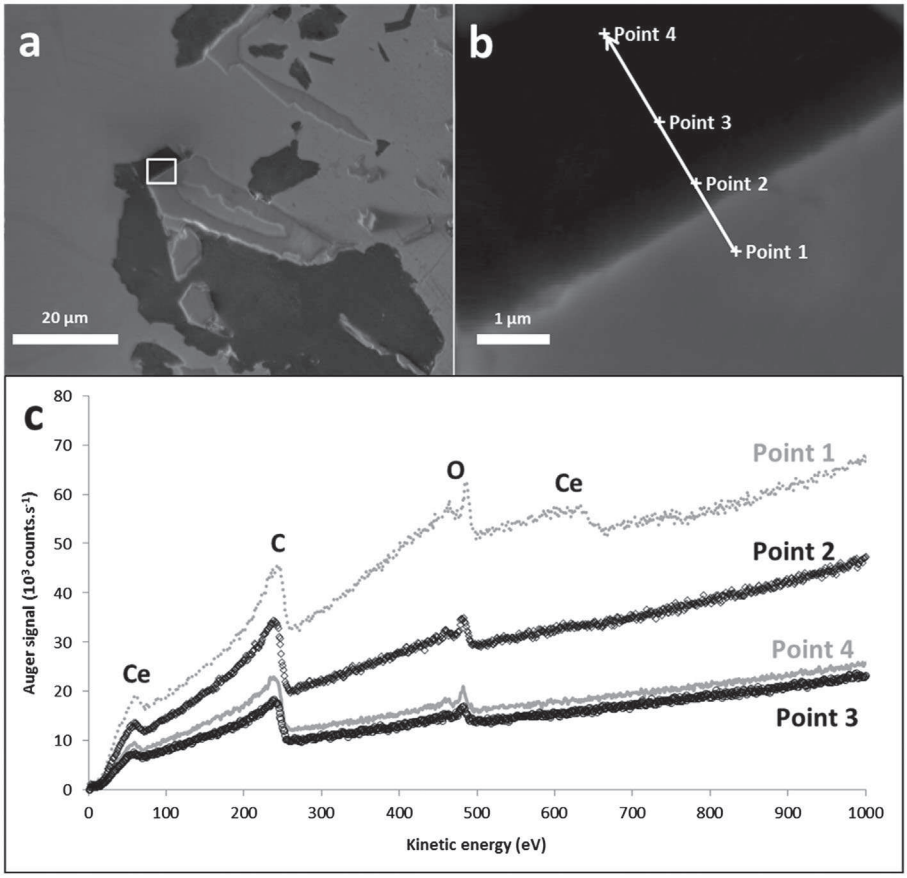

4 SEM image of a graphite precipitate attached to a Ce-rich precipitate *a* investigated points *b* and corresponding Auger spectra *c*

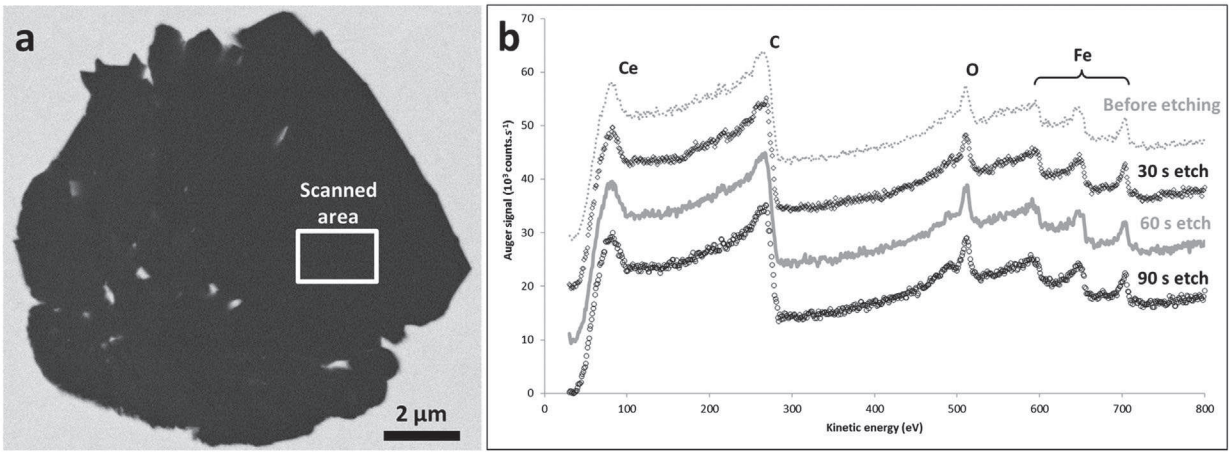

5 SEM image of an investigated area in a graphite precipitate *a* and corresponding Auger spectra *b*

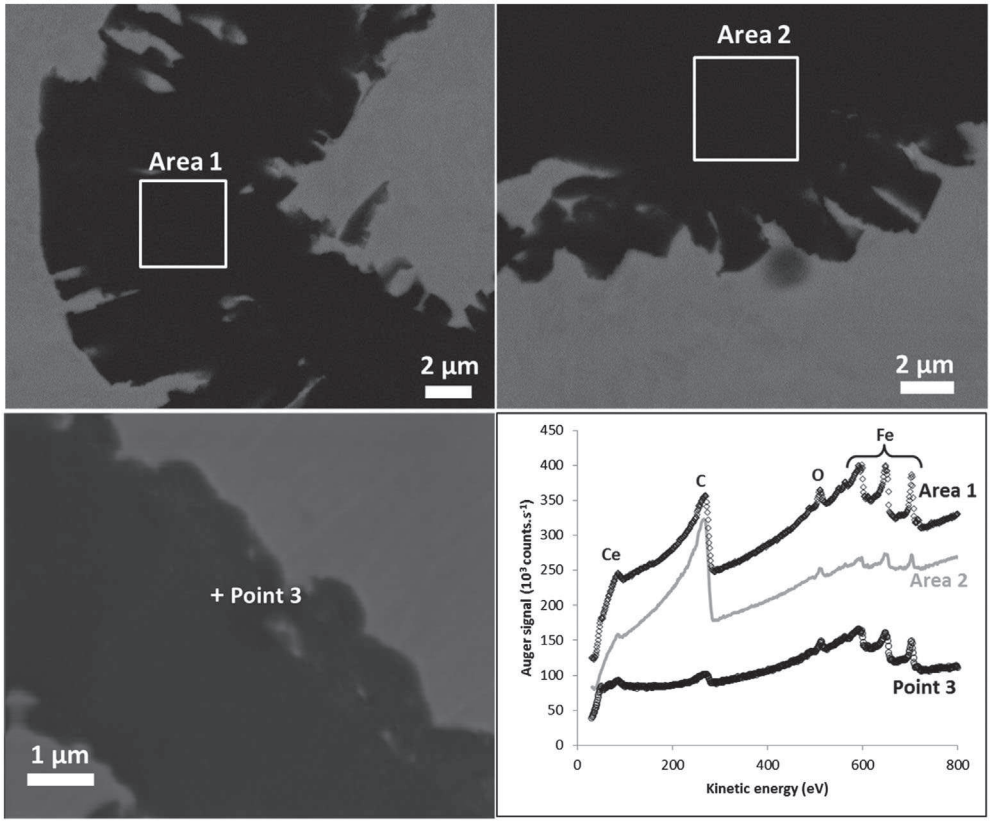

6 Detection of cerium, iron and oxygen in degenerate graphite precipitates

intercalated in the graphite lattice and promote growth defects.[14,15] In the present work cerium and oxygen peaks were always observed together when analysing degenerate graphite precipitates, but only in limited instances could the presence of cerium oxide be ascertained. In general terms, these observations do anyway support growth models involving incorporation of foreign elements into the graphite lattice. The detailed mechanism for spheroidal graphite growth is however still under debate. The possibility of growth around screw dislocations has been disregarded following TEM examination of graphite orientations along sectors of well-formed spheroids.[16] However, observation of exploded graphite suggested spheroidal growth results from continuous nucleation of new graphite units at the outer surface of the spheroid, which then grow on top the spheroid surface along the graphite prismatic direction.[17]

Conclusions

Scanning Auger microscopy was used to investigate graphite precipitates in an Fe-C-2%Ce alloy and showed no accumulation of any elements at the interfaces between graphite precipitates and the matrix. Cerium was found to be combined with oxygen in confined areas such as matrix intrusions at the periphery of graphite spheroids, in the form of discrete Ce_xO particles and not as a boundary interlayer. The presence of cerium in the bulk of spheroidal graphite precipitates has been observed on occasions, but it cannot yet be determined whether this is a requirement for spheroidal growth. It is quite possible

that in locations where Ce was not detected, this element was present at an amount below the detection limit of Auger electron spectroscopy. Furthermore, cerium, iron and oxygen were detected in several degenerate graphite structures suggesting a possible link between Ce content and graphite degeneracy. Quantitative information would be necessary to pursue work in this line of thought. Comparing peak intensities of the sample to those of pure standards should be considered in further investigations. Nevertheless, careful selection of acquisition parameters and methodology is required as quantitative interpretation of Auger signals can lead to inaccurate results.[18] For such purposes, Auger mapping using the snapshot acquisition mode could be used since it has the advantage of limited time duration, while associated to standards it could lead to the determination of absolute Ce composition mapping.

References

1. M. Hillert and Y. Lindblom: 'The growth of nodular graphite', *J. Iron Steel Inst*., 1954, **148**, 388–391.
2. M. Olette, A. Kohn and P. Kozakevitch: 'Contribution à l'étude du mécanisme de formation du graphite primaire dans les fontes', *Fonderie*, 1965, **229**, 87–99.
3. I. Minkoff and W. C. Nixon: 'Scanning Electron Microscopy of Graphite Growth in Iron and Nickel Alloys', *J. Appl. Phys*., 1966, **37**, 4848–4855.
4. J. Lacaze, N. Valle, K. Theuwissen, J. Sertucha, B. El Adib and L. Laffont: 'Distribution and effect of various doping elements during primary graphite growth in cast iron', *Adv. Mater. Sci. Eng.*, 2013, paper ID 638451.
5. W. Johnson and H. Smartt: 'The role of interphase boundary adsorption in the formation of spheroidal graphite in cast iron', *Metall. Trans. A*, 1977, **8**, 553–565.
6. J. D. Verhoeven, A. J. Bevolo and J. S. Park: 'Effect of Te on morphological transitions in Fe-C-Si alloys: Part II. Auger analysis', *Metall. Mater. Trans. A*, 1989, **20**, 1875–1881.
7. K. Theuwissen, J. Lacaze, L. Laffont, J. Zollinger and D. Daloz: 'Effect of Ce and Sb on primary graphite growth in cast irons', *Trans. Indian Inst. Met.*, 2012, **65**, 707–712.
8. S. E. Franklin and R. A. Stark: 'Application of secondary ion mass spectrometry to study of graphite morphology in cast iron', *Metal Sci.*, 1984, **18**, 187–200.
9. S. E. Franklin and R. A. Stark: 'Further use of secondary ion mass spectrometry in the study of graphite morphology control in cast irons', in 'The Physical Metallurgy of Cast Irons', Vol. 34, 'MRS Symposia Proc.', 1985, 25–35.
10. D. D. Double and A. Hellawell: 'The nucleation and growth of graphite-the modification of cast iron', *Acta Metall. Mater*., 1995, **43**, 2435–2442.
11. B. Lux: 'On the theory of nodular graphite formation in cast iron- Part I: experimental observations of nodular graphite formation during the solidification of cast iron melts', *Giessereifoschung in English*. 1970, **22**, 65–81.
12. H. Fidos: 'A study of the graphite morphology in nodular cast iron', *FWP J.*, 1977, **17**, 39–54.
13. H. Fidos: 'Structural analysis of a graphite nodule and surrounding halo in ductile iron', *FWP J*., 1982, **22**, 43–62.
14. G. R. Purdy and M. Audier: 'Electron Microscopical Observations of Graphite in Cast Irons', in 'The Physical Metallurgy of Cast Irons', Vol. 34, 'MRS Symposia Proc.', 1985, 13–23.
15. B. Miao, K. Fang, W. Bian and G. Liu: 'On the microstructure of graphite spherulites in cast irons by TEM and HREM', *Acta Metall. Mater*., 1990, **38**, 2167–2174.
16. Theuwissen K., Lafont M.-C., Laffont L., Viguier B. and J. Lacaze: 'Microstructural characterization of graphite spheroids in ductile iron', *Trans. Indian Inst. Met*., 2012, **65**, 627–631.
17. R. Ghergu, L. Magnusson Aberg and J. Lacaze: 'A possible mechanism for the formation of exploded graphite in nodular cast irons', *Mater. Sci. Forum*, 2014, **790–791**, 435–440.
18. R. Kosiba, J.Liday, G. Ecke, O. Ambacher, J. Breza and P. Vogrincic: 'Quantitative Auger electron spectroscopy of SiC', *Vacuum*, 2006, **80**, 990–995.